Effect of density ratio on the performance of purge flow in linear cascade arrangement

Kamil Abdullah, Haswira Hassan and Muzzammil Pauzi
Center for Energy and Industrial Environment Studies, Universiti Tun Hussein Onn Malaysia, Parit Raja, Johor, MALAYSIA

Corresponding author: mkamil@uthm.edu.my

Abstract. Purge flow has been recognized as potential solution to provide cooling protection at the end wall region of a turbine blade arrangement. The present paper investigates the effects of density ratio on the performance of purge flow in linear cascade arrangement. Computational fluid dynamics has been manipulate to investigate the pressure loss coefficient and the film cooling effectiveness produces by purge flow at three different density ratio value. Two mass flow rate of the purge have been considered in the present study. The investigation indicates no influence of density ratio on aerodynamic losses of the purge flow however petite improvement in terms of area average film cooling effectiveness have been observed at higher density ratio value.

1. Introduction

Gas turbines have been widely use today's power generation and transportation sectors. The efficiency of a gas turbine can be improved by increasing the turbine inlet temperature (TIT). Since its introduction in 1930s, the TIT had been increased from 540 °C in the conventional gas turbines to 1425 °C and higher in the modern gas turbines [1]. At these temperatures, sophisticated cooling scheme is required to ensure turbine components operational durability. Among the existing cooling technique which commonly found in gas turbine system are, film cooling, internal cooling, and purge flow cooling. These cooling techniques are essential to provide thermal protections to the turbine components especially at the critical area such as blade end-wall region [2]. In addition to the film cooling, purge flow cooling has also been considered to provide thermal protection for end-wall regions. Purge flow make used of compress air that leaks through the space of between the rotor and stator joints to cool the end wall region. Among parameters that influence the purge cooling performance are mass flow ratio, density ratio, Reynolds number and blade profile.

In visualizing the complex flow structure at the end wall, Takeshi et al. [3] carried out an experiment to capture and understand the blade end-wall flow structure. The study reveals that it consists of pressure side and suction side horse-shoe vortex, cross flow, corner vortex and passage vortex as shown in Figure 1. Among the early experimental study on end-wall cooling and hydrodynamics is by Blair [4] which relates the end-wall flow structure and its thermal protection capabilities. The study clarifies that heat transfer of film cooled end-wall is significantly influenced by the horse-shoe vortex and passage vortex. Other works such as Gao et al. [5] and Narzary [6] have tested a typical labyrinth-like stator-rotor seal under different blowing conditions. The works focus on the thermal protection capability of the purge flow without providing any information on the aerodynamic performance. Barigozzi et al. [7] have discussed the performances of purge flow through

a rotor blade cascade arrangement. The study take into consideration of both the aerodynamics and thermal performance of purge flow at various mass flow ratio (MFR) involving experimental and simulation work. One of the latest study on the purge flow cooling is by Wan Ghopa et al. [2]. The study highlights the influence of purge flow on aerodynamics performance in high-pressure turbine cascade at various MFR values. The study has made used as experimental and numerical method with good agreements between those two methods have been reported.

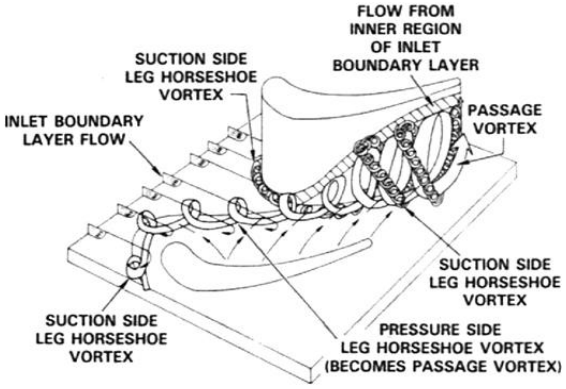

Figure 1. Complex flow structure at the end-wall area

The present study aims to extend the work of Wan Ghopa et al. [2] with considering mainly investigates the purge flow used to shield and protect the vane platform from the hot mainstream gas. The study will focus on the effect of density ratio to the aero-thermal performance of the purge flow cooling.

2. Methodology

2.1. Computational domain

The present study is considering two different computational domains; no-purge and with-purge computational domains. The no-purge domain will provides the baseline results at MFR = 0.0 for aerodynamics and thermal performance of the given blade profile. The with-purge domain will be use to provides results for MFR > 0.0. The blade profile and geometry is the same with the one used by Wan Ghopa et al. [2] as shown in Figure 2 and Table 1.

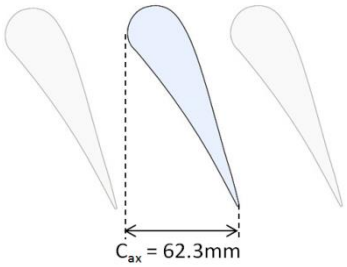

Figure 2. Blade geometry and arrangement

Table 1. Geometrical details of the blade

	Distance	
Chord length, C	12.2 mm	@ 0.196Cax
Axial chord, C_{ax}	62.3 mm	@ Cax
Blade pitch, p	115.9 mm	@ 1.680Cax
Blade height, s	117.68 mm	@ 1.889Cax

The computational domains have been made of structured mesh for the entire domain. The near wall region has been constracted to meet the requirement of $y+$ equal to unity with the total number of nodes is at 4,923,280 nodes. Figure 3 shows details of the mesh topology involved in the present study. The present numerical investigations were carried out using ANSYS CFX software. Reynolds

Average Navier Stokes analysis was applied with the employment of Shear Stress Transport turbulence model. The boundary conditions applied in the present study is as in Table 2.

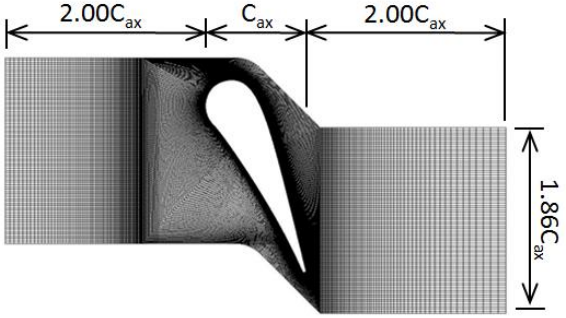

Figure 3. Mesh topology and computational domain dimension

Table 2. Boundary conditions

Flow Parameter	Value
Mainstream pressure [Pa]	1752
Mainstream Temp. [C]	37
Purge Flow Temp. [C]	85, 66, 48
MFR [%]	0.6, 1.2
Density Ratio	0.85, 0.90, 0.95

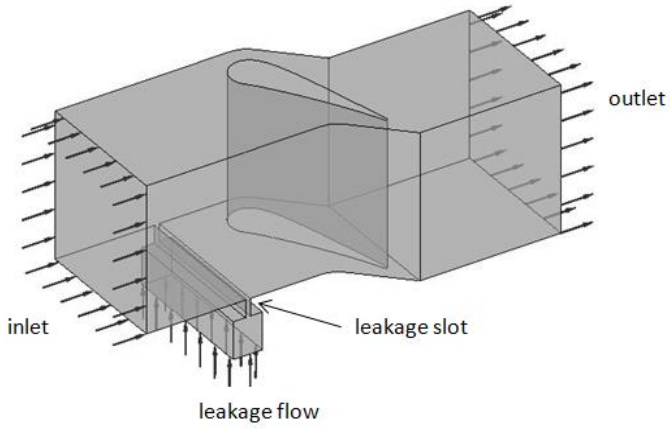

Figure 4. Overview of the computational domain together with the applied boundary conditions

2.2. Performance indicator

In the present study, the influence of the purge flow towards aerodynamics and thermal performance is evaluated through total pressure loss coefficient and film cooling effectiveness respectively. The total pressure loss coefficient indicates the energy flow loss relative to the incoming energy brought by the mainstream flow. Eq. (1) shows the formula for total pressure loss coefficient, C_{pt} where P_{ti} is inlet total pressure [Pa], P_{to} is outlet total pressure [Pa], ρ is the density of the fluid [kg·m^{-3}] and V_2^{∞} is inlet velocity [m·s^{-1}].

$$C_{pt} = \frac{(P_{ti} - P_{to})}{\frac{1}{2}\rho V_{\infty}} \quad (1)$$

In addition, the thermal performance is measure through film cooling effectiveness, η given by Eq. (2) where, T_{aw} is adiabatic wall temperature (°C), T_{∞} is main flow temperature (°C) and T_2 is secondary air temperature (°C). The highest η value of unity represents maximum utilization of the secondary air in providing thermal protection to the surfaces and the lowest value of zero represent no thermal protection provided by the secondary air.

$$\eta = \frac{(T_{aw} - T_{\infty})}{(T_s - T_{\infty})} \quad (2)$$

2.3. Mesh dependency test

To evaluate the mesh dependency test of the solution, meshes have been tested with coarser, 3.5 million, 4.9 million and 7.1 million of elements. Velocity profile at upstream of the leakage slot has been taken to be evaluated. The evaluation concludes that the number of elements used in the present study is 4.9 million.

3. Result and discussion

3.1. Aerodynamic loss

Figure 5 shows the results of pressure loss coefficients contour at different mass flow ratio on YZ planes located at 1.25 C_{ax}. The losses contour is taken at density ratio of 0.9 with other density ratio recorded similar pattern. The figure indicates a core of losses allocated at y/p = 0.5 followed by a clear losses region in z-axis direction. The losses recorded for MFR = 1.2 is higher in comparison with the case of MFR = 0.6. The losses core is generated by the interaction between the passage vortex and horseshoe vortex as been shown earlier in Figure 1. The figure also indicates that the losses is more concentrated for the case of MFR = 1.2. This is due to the strength of the horseshoe vortex which is directly associated with the amount of leakage flow introduced into the mainstream flow path. In terms of end wall losses, the higher losses produced at higher MFR can be observed clearly from the figure. The end wall losses pattern at MFR = 1.2 is skewed toward the blade wall indicates a stronger momentum of the leakage flow introduced through the slot. Similar discussion can be made for the other density ratio values.

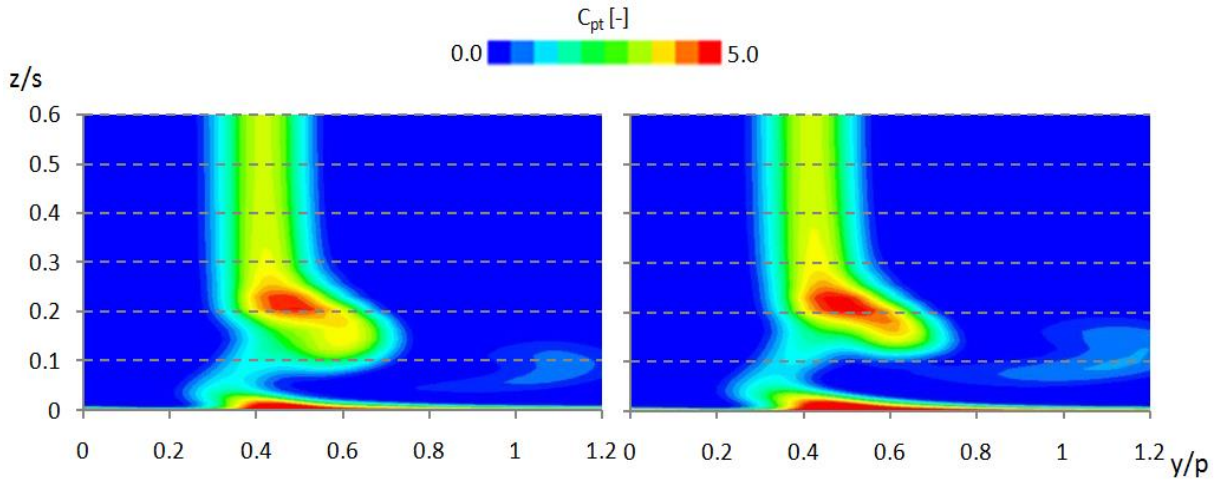

Figure 5. Loss coefficient contour plot for MFR = 0.6 and 1.2 at C_{ax} = 1.25

Figure 6 shows the total loss coefficient for all considered cases. The figure clearly indicates that density ratio does not have any influence on the aerodynamic losses with constant losses have been recorded throughout the density ratio values. The figure also confirms the higher losses recorded at MFR = 1.2 as been discussed earlier in the previous section. Quantitatively, the losses recorded at MFR = 1.2 is 4% higher than the losses recorded for the case MFR = 0.6.

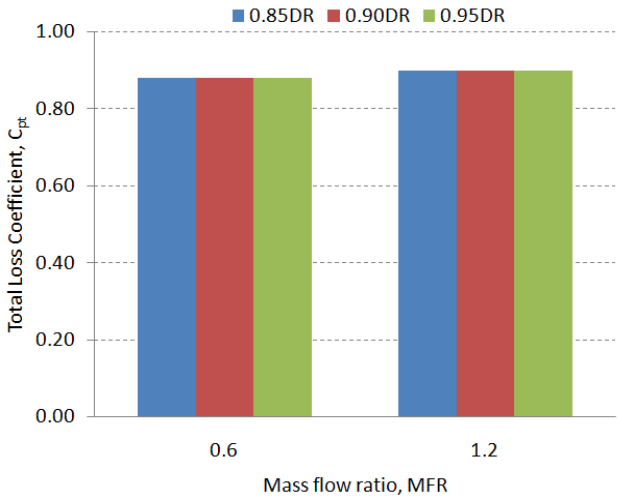

Figure 6. Total loss coefficient of all considered density ratios and mass flow ratio

3.2. Film cooling effectiveness

Figure 7 shows the results of film cooling effectiveness distribution on the end wall for two different MFR values at 0.6 and 1.2. The results are taken for the case density ratio of 0.9 due to similar distribution pattern that have been observed at different density ratio value. Generally the figure indicates better film cooling effectiveness coverage at lower MFR value in comparison with higher MFR value. This is due to the lower momentum at lower MFR value allows the leakage flow to remain attached to the end wall surface. At higher MFR value, the momentum of the leakage flow induces stronger vortex structure penetrating the mainstream flow path leaving the end wall area unprotected. In addition to that, the strong vortex structure penetrating the mainstream flow also more vigorous interaction between the leakage flow and the mainstream air causes the leakage flow to lose its cooling capability at much faster rate. The figure also indicates the uncovered area of the blade leading edge.

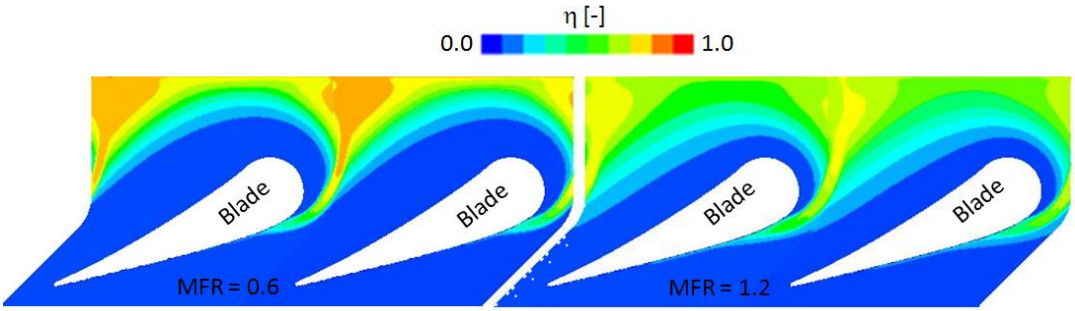

Figure 7. Film cooling effectiveness contour plot for MFR = 0.6 and 1.2

The origin of higher film cooling effectiveness path illustrated in the figure is also the same origin of the suction side horseshoe vortex. The vortex bring together high concentration of leakage flow allowing the establishment of high film cooling effectiveness from the leakage slot to the suction side of the blade. Although MFR = 1.2 show a much more lower concentration of film cooling effectiveness, the higher momentum of the leakage flow allow wider coverage of the leakage flow in comparison with lower MFR cases.

Figure 8 shows the area average film cooling effectiveness for all considered cases. The figure clearly indicates higher area average film cooling effectiveness in the case of higher MFR. Although the concentration of film cooling effectiveness is lower at higher MFR, the coverage area of the leakage flow is wider due to the capability of the leakage flow to spread through the end wall region.

Numerically the area average film cooling effectiveness at MFR = 1.2 is 15% higher in comparison with the case MFR = 0.6. The figure also indicates improvement in terms area average film cooling effectiveness at higher density ratio although might not significant.

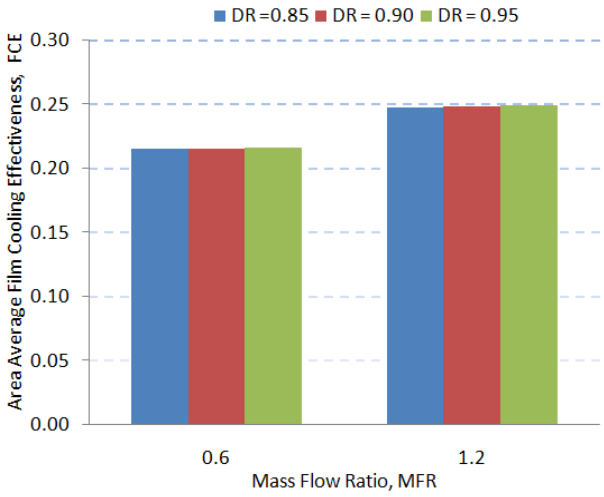

Figure 8. Area average film cooling effectiveness of all considered density ratios and mass flow ratio

4. Conclusion

Investigation on the effect of density ratio on the performance of purge flow in linear cascade of stator blade arrangement has been carried out in the present study. Overall of six cases have been considered involving three different density ratio at two different mass flow ratio. Based on the results obtained, the listed conclusions can be made are:

1. The flow behaviour on the end wall region is significantly influenced by the secondary flow structure involving horseshoe vortex at both the suction and the pressure side of the balde.
2. The leading edge region is unprotected by the leakage flow due to the formation of the passage vortex.
3. Higher MFR produces higher aerodynamic losses due to the formation of the passage vortex.
4. Density ratio has no significant effect in terms of aerodynamic losses.
5. Lower MFR produces higher concentration of film cooling effectiveness but provide less area coverage in comparison with higher MFR.
6. Area average film cooling effectiveness of higher MFR is better than the lower MFR case.

Acknowledgement

The author would like to thank both Universiti Tun Hussien Onn Malaysia (UTHM) and Ministry of Higher Education of Malaysiafor the financial support through Fundamentals Research Grant Scheme (Vot 1544).

Reference

[1] Yunus A. Cengel & Michael A. Boles (2011) Thermodynamic: An Engineering Approach, 7th edition, McGraw-Hill, 503-506.
[2] Wan Aizon W. G., Funazaki K. & Miura T. (2013) Purge Flow Effect on Aerodynamics Performance in High-Pressure Turbine Cascade, Journal of Mechanical Science and Technology, 1611-1617.
[3] Takeishi K., Matsuura M., Aoki S. & Sato T. (1990), An Experimental Study of Heat Transfer and Film Cooling on Low Aspect Ratio Turbine Nozzles, ASME Paper No. 89-GT-187, ASME Journal of Turbomachinery, 112 488-496.

[4] Blair M. F. (1974), An Experimental Study of Heat Transfer and Film Cooling on Large-Scale Turbine Endwalls, ASME Journal of Heat Transfer, 96 524-529.
[5] Gao Z., Narzary D. & Han J. C. (2009), Turbine Blade Platform Film Cooling with Typical Stator-Rotor Purge Flow and Discrete-Hole Film Cooling, Journal of Turbomachinery, 131.
[6] Narzary D. (2009), Experimental Study of Gas Turbine Blade Film Cooling and Heat Transfer, PhD Dissertation, Texas A&M University, August 2009.
[7] Barigozzi G., Fontaneto F., Franchini G. & Perdichizzi A. (2012), Aero-Thermal Performances of a Rotor Blade Cascade with Stator-Rotor Seal Purge Flow, Proceedings of ASME Turbo Expo 2012, June 11-15, Copenhagen, Denmark.